Taylor & Francis
Taylor & Francis Group

ORIGINAL RESEARCH

🔓 OPEN ACCESS   Check for updates

Metabolic heterogeneity in tumor cells impacts immunology in lung squamous cell carcinoma

Qian Wang[a]*, Na Sun[a]*, Chaoyang Zhang[a], Thomas Kunzke[a], Philipp Zens[b,c], Annette Feuchtinger[a], Sabina Berezowska[b,d], and Axel Walch[a]

[a]Research Unit Analytical Pathology, Helmholtz Zentrum München - German Research Center for Environmental Health, Neuherberg, Germany; [b]Institute of Tissue Medicine and Pathology, University of Bern, Bern, Switzerland; [c]Graduate School for Health Sciences, University of Bern, Bern, Switzerland; [d]Department of Laboratory Medicine and Pathology, Institute of Pathology, Lausanne University Hospital and University of Lausanne, Lausanne, Switzerland

ABSTRACT

Metabolic processes are crucial in immune regulation, yet the impact of metabolic heterogeneity on immunological functions remains unclear. Integrating metabolomics into immunology allows the exploration of the interactions of multilayered features in the biological system and the molecular regulatory mechanism of these features. To elucidate such insight in lung squamous cell carcinoma (LUSC), we analyzed 106 LUSC tumor tissues. We performed high-resolution matrix-assisted laser desorption/ionization (MALDI) mass spectrometry imaging (MSI) to obtain spatial metabolic profiles, and immunohistochemistry to detect tumor-infiltrating T lymphocytes (TILs). Unsupervised k-means clustering and Simpson's diversity index were employed to assess metabolic heterogeneity, identifying five distinct metabolic tumor subpopulations. Our findings revealed that TILs are specifically associated with metabolite distributions, not randomly distributed. Integrating a validation cohort, we found that heterogeneity-correlated metabolites interact with CD8+ TIL-associated genes, affecting survival. High metabolic heterogeneity was linked to worse survival and lower TIL levels. Pathway enrichment analyses highlighted distinct metabolic pathways in each subpopulation and their potential responses to chemotherapy. This study uncovers the significant impact of metabolic heterogeneity on immune functions in LUSC, providing a foundation for tailoring therapeutic strategies.

Background

Metabolic reprogramming is a hallmark of cancer,[1] leading to heterogeneous and complex metabolic profiles that complicate metabolic-targeted therapies. These alterations are closely linked to immune cell functions within the tumor microenvironment (TME).[2] Recent research highlights the intricate interplay between metabolic processes and immune functions,[2–4] with dysregulation of these pathways associated with chronic inflammatory disorders and cancers.[5–7] Metabolic pathways unexpectedly regulate T-cell fate, function, and differentiation,[8] but the complexity of immunometabolic reprogramming in diseases remains poorly understood due to disease heterogeneity and diverse phenotypes. The TME's unique immune and metabolic characteristics reprogram cell-cell communication and alter antitumor responses.[9] Given that tumors rely on metabolites for growth and T cells must substantially increase nutrient uptake to mount a proper immune response, investigating the association between metabolic heterogeneity and immune functions could uncover potential crosstalk or competition within the TME, further revealing novel strategies to inhibit tumor growth while enhancing anti-tumor immunity.

Tumor heterogeneity is a significant challenge in cancer diagnosis and treatment, manifesting as genetic, metabolic, TME,[10–13] and other heterogeneity. Studies across various cancer types indicate that intratumoral heterogeneity drives tumor progression and fosters drug resistance, including in lung cancer.[14] Lung cancer, the leading cause of cancer-related death globally,[15] is predominantly non-small-cell lung cancer (NSCLC), with about 30% being lung squamous cell carcinoma (LUSC).[16,17] Studies in NSCLC patients revealed that intratumoral heterogeneity varies with mutational burden, and low mutational burden was correlated with better overall survival.[18,19] Single-cell RNA sequencing further showed that LUSC has greater inter- and intratumor heterogeneity than lung adenocarcinoma.[20] These findings underscore the importance of studying factors like metabolic heterogeneity in lung cancer.

Immunometabolism bridges metabolism with immunology at both intracellular and whole-body levels.[21] Studying tumor immunometabolism requires techniques that capture metabolic heterogeneity in TME. Mass spectrometry imaging (MSI) is a key method, enabling direct, systematic quantification of metabolism in intact cell populations.[22] MSI has

provided insights into the metabolic underpinnings of lung cancer, aiding molecular classification strategies.[23,24] Matrix-assisted laser desorption/ionization (MALDI) is the most common approach in spatial metabolomics, allowing in situ screening of molecular classes within their histopathological context.[25–27] High cellular specificity of MSI has proven effective in identifying predictive biomarkers.[24,28,29] Identifying molecular alterations within tumor tissues and underlying immunometabolism offers insights into biochemical heterogeneity and the role of metabolic reprogramming in cancer. Immunohistochemistry (IHC) complements this by identifying tumor-infiltrating T lymphocytes (TILs) and other immune markers, which can be predictive and prognostic.[30–34] Exploring the spatial distribution of immune cells and their interactions with cancer and stromal cells may enhance our understanding of cancer progression.[35]

In this study, we integrated spatial metabolomics with unsupervised k-means clustering and Simpson's diversity to investigate tumor-specific metabolic heterogeneity and interactions in the LUSC immune microenvironment. Using MALDI-MSI, we mapped spatially resolved metabolites across tumor regions in clinically annotated samples. We assessed metabolic heterogeneity and identified distinct tumor subpopulations with unique metabolic activities and chemotherapy responses. We found significant associations between TILs and both metabolic heterogeneity and tumor subpopulations. Combining these findings with genomics data, we identified genes correlated with TILs, specific metabolites, and patient survival. This study offers new insights into the cross-talk between immune cells and tumor metabolic heterogeneity in LUSC.

Materials and methods

Patient cohort and tissue samples

Tumor samples were obtained from 106 LUSC patients (Table 1) diagnosed at the Institute of Pathology, University of Bern, excluding cases with prior or concurrent LUSC in other organs. A tissue microarray (TMA) was constructed from formalin-fixed and paraffin-embedded (FFPE) tissue blocks.

Table 1. Patient characteristics.

Clinicopathological characteristics of the LUSC cohort	
Characteristic	Number
Total LUSC patients	106
Sex	
male	95
female	11
Age (years): median (range)	69 (43–85)
Tumor size (mm): median (range)	45 (8–130)
UICC stage	
I	37
II	32
III	33
IV	4
Distant metastases	
M0	102
M1	4
Primary resection	
R0	91
R1	15

High mass resolution MALDI Fourier-transform ion cyclotron resonance (FT-ICR) MSI

Briefly, the FFPE section (4 µm) was mounted onto indium tin oxide-coated glass slides. The air-dried tissue section was spray-coated with 10 mg/mL 9-aminoacridine (9-AA) hydrochloride monohydrate matrix in 70% methanol. Prior to matrix application, the FFPE tissue section was deparaffinized in xylene. Metabolite detection was performed in negative ion mode. Mass spectra were acquired in the range of *m/z* 50–1,100 with a lateral resolution of 50 µm.

Unsupervised pixel-wise k-means segmentation and metabolic tumor subpopulation determination

Using the segmentation tool in Bruker SCiLS Lab, unsupervised k-means clustering was performed pixel-wisely containing overall resolved MS peaks within only tumor regions with k range from 2 to 15. For further statistical analysis, we linked the survival data of patients to the presence of specific clusters and consequently determined the metabolic tumor subpopulations (MTSs). The fitness of the model at each k was assessed using the Akaike information criterion (AIC) involving patients' overall survival; the model with the lowest AIC value was presumed to most closely fit the data. Applying the k value and threshold of pixels fraction corresponding to the lowest AIC value, patients were assigned to certain clusters, so-called MTSs. Specifically, each MTS stands for a LUSC patient cluster with certain tumor-specific metabolic profiling and features.

Simpson's diversity index as heterogeneity score

The calculation formular Simpson diversity index measures in our study is defined as follows:

$$D = 1 - \sum_{i=1}^{k} p_i^2,$$ where p_i is the share of pixels in cluster i and k is the number of clusters.

The formular is built considering the spatial locations of pixels for each patient in each cluster. Each pixel is located by x and y coordinates which were extracted from SCiLS Lab software. The index can have values between 0 and 1. A value of 0 means that all the pixels from one patient are in one cluster. A higher value of the index, therefore, indicates higher diversity of the pixels in the different clusters for a patient. As the heterogeneity score for each patient, the Simpson index to measure the metabolic heterogeneity of the patients is calculated using the within sum of squares as entries p_i. A higher heterogeneity score stands for a higher metabolic heterogeneity level.

More details of materials and methods can be found in the Supplementary file.

Results

Identification of MTSs in LUSC

The study design and pipeline are shown in Figure 1a. Supplementary Fig. S1A represents the high-resolution IHC images of immunological markers analyzed in this study. Supplementary Fig. S1B displayed the distinguished
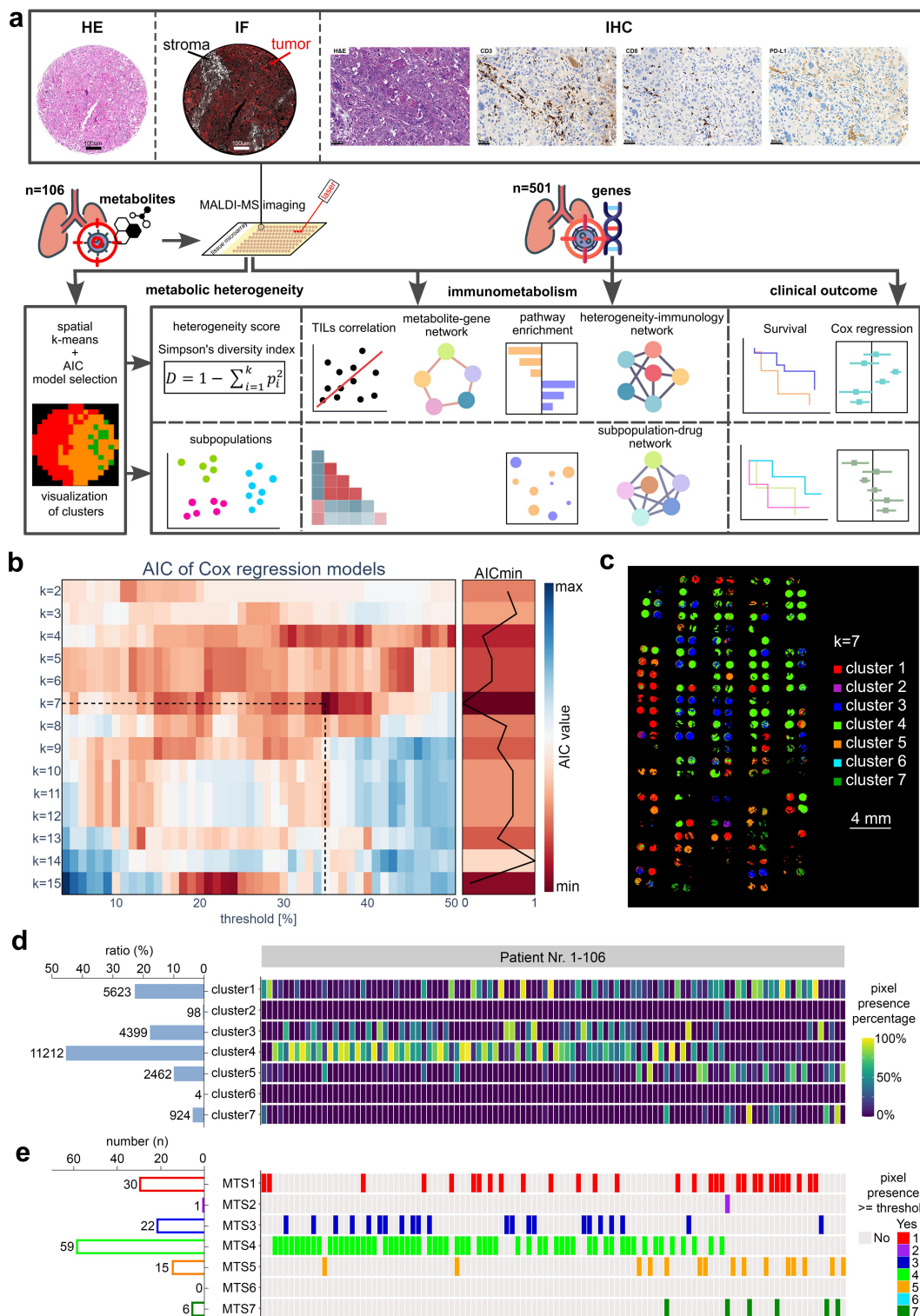
Figure 1. Unsupervised *k*-means clustering of tumor-specific spatial metabolomics data from 106 patients with LUSC. (A) The top part shows the example images from HE, IF and IHC experiments, respectively, indicating how the tumor regions were annotated and immunological features were measured. The bottom part illustrated the complete study design including the spatial metabolomics experiment and analysis approaches. (B) AIC model selection criteria indicated that *k* = 7 fitted the data the best with a threshold 35% of pixels presence. The left heatmap shows the AIC values at different thresholds as the *k* value changes. The minimum AIC values from each *k* are scaled to 0–1 and visualized as a line graph in the right heatmap to facilitate comparison. (C) Spatial segmentation map of k7 clustering results in LUSC tissue samples. (D) Pixels distribution of 106 tumor ROIs in 7 clusters. The heatmap on the right shows the percentages of pixels presences of each tumor ROI in different clusters; the bar chart on the left shows the number of each cluster's pixels, of which the length of the bar indicates the percentages of total pixels and the number indicates the absolute count. (E) Patients distribution in MTSs. The heatmap on the right shows the patients with pixels above the pixel presence threshold; the bar chart on the left shows the number of patients in each MTS.

distributions of three typical metabolites in all patient tissues. Via the comparison of the minimum AIC values at each k, $k = 7$ with a threshold of 35% showed the lowest AIC value across all k values and thresholds, and was thus defined as the optimal value for the number of clusters and the threshold (Figure 1b). One patient could be segmented into more than one cluster (Figure 1c), which was due to the high metabolic heterogeneity of the patients. The spatial pixel distribution of overall peaks from 106 LUSC patients in 7 clusters were quantified as percentages and visualized in Figure 1d. In order to determine the clinical importance of each metabolomics cluster, the results of the metabolite segmentation had to be linked to the clinical data of the patients. By comparing with the AIC-guided threshold of 35% pixel presences, 106 LUSC patients were assigned to MTS1 ($n = 30$), MTS2($n = 1$), MTS3 ($n = 22$), MTS4 ($n = 59$), MTS5 ($n = 15$) and MTS7 ($n = 6$); as each of patients in MTS6 held < 35% of the pixels, there was no patient were assigned (Figure 1e). To achieve robust and substantial results, MTS2 ($n = 1$) was also excluded from the further analyses in the consideration of statistical principle.

Metabolic heterogeneity was associated with immunological landscapes and showed an independent prognostic value

To further compare the heterogeneity status of individual patients, Simpson's diversity index was applied to quantify each patient with an index value. The index distribution shown in Figure 2a indicated a diversity among patients' heterogeneity. As metabolic heterogeneity increased, the correlation of heterogeneity with the metabolic pathways of nicotinate and nicotinamide metabolism, pyrimidine metabolism as well as tryptophan metabolism enhanced, while the correlation with the metabolic pathways of steroid hormone biosynthesis, amino sugar and nucleotide sugar metabolism, pantothenate and CoA biosynthesis as well as cysteine and methionine metabolism weakened (Figure 2b). By correlating Simpson index to the expression of immunological markers, we found that the patients with higher Simpson index tended to have lower CD3 + and CD8+ TILs, while the expression of PD-L1 didn't show a significant correlation (Figure 2c). Metabolites usually interact with genes to regulate immune responses through a complex network of interactions. Integrative analyses, such as genomics, transcriptomics, proteomics, and metabolomics, help understand such kind of complex interactions. For that, by integrating the genomics data from a validation LUSC cohort ($n = 501$) into our analysis, we identified 27 genes that may have functions in human by interacting with heterogeneity-correlated metabolites and meanwhile positively correlated with CD8+ TIL infiltration level in LUSC patients (Figure 2d & Supplementary Fig. S2). Those heterogeneity-correlated metabolites include five negatively correlated ones and three positively correlated ones. Among the 27 infiltration-related genes, the LUSC patients with high expression of endoplasmic reticulum auxin binding protein 1 (*ABP1*), phospholipase A2 group IB (*PLA2G1B*) and snail family zinc finger 1 (*SNAI1*) led to a worse overall survival (Figure 2d). Phosphatidylcholines (PC) as a metabolite that negatively associated with heterogeneity score were found to

have an unfavorable impact on the PFS of LUSC patients in our study (Figure 2d).

Based on Simpson's diversity index, 30 patients were stratified as high heterogeneity and 76 patients were as low heterogeneity (Figure 3a). The Kaplan-Meier curves revealed that LUSC patients with high heterogeneity had significantly worse overall survival (Figure 3b) and progression-free survival (Figure 3c) compared to LUSC patients with low heterogeneity. Meanwhile, the patients with high CD3+ or CD8+ TIL were found to have better progression-free survival (Figure 3d,e). Importantly, by multivariate Cox analysis, we found that the impact of metabolic heterogeneity on survival was stronger than the impact of TILs and independent (Figure 3f,g). Given the negative correlation between metabolic heterogeneity with TILs, the metabolites co-abundant with CD3+ and CD8+ TILs in LUSC patients were identified to explore their roles in immune processes. The metabolite-immune network displayed that, the co- abundant metabolites in high heterogeneity mainly take part in the immune process of neutrophil and memory B cell; while in low heterogeneity mainly the immune process of erythrocyte, granulocyte, and microglia (Figure 3h). Basophil activation was a shared correlated immune process in both high- and low-heterogeneity (Figure 3h).

The correlations of metabolic heterogeneity levels with clinicopathological features were investigated as shown in Figure 4a. To rule out potential confounding interaction between metabolic heterogeneity levels and clinicopathological features, we performed multivariate Cox analysis for PFS and OS (Figure 4b). High metabolic heterogeneity, high UICC stages, and age equal or above 70 years old had a significantly unfavorable impact on OS and PFS. Other co-factors (sex, tumor size, distant metastases, and primary resection) did not affect PFS or OS (Figure 4b).

MTSs were independent factors for survival and associated with TILs

Followed by linking the clinical data of LUSC patients to the AIC-threshold MTSs, statistically significant differences in OS ($p = 0.019$) were found between MTSs (Figure 5a), but not in PFS ($p = 0.250$) (Figure 5b). In the pairwise comparisons for OS, statistically significant differences were observed between MTS1 versus MTS3 ($p = 0.042$), MTS4 versus MTS5 ($p = 0.021$), and MTS3 versus MTS5 ($p < 0.001$), respectively (Figure 5c–e). In the pairwise comparisons for PFS, statistically significant differences were observed between MTS3 versus MTS5 ($p = 0.027$) (Figure 5f). We next assessed the distributions of Simpson index and heterogeneity levels among MTSs, which indicated diversity of their heterogeneity (Figure 5g,h). Correlation analysis then was used to investigate the immunological and clinical features of each MTS (Figure 5I,J). MTS1 was positively correlated with CD3+ TIL, CD8+ TIL and tumor size. MTS3 was negatively correlated with age and primary resection status. MTS4 was positively correlated with CD3+ TIL and CD8+ TIL while negatively correlated with tumor size. MTS7 was positively correlated with PD-L1 and UICC stages while negatively correlated with primary resection status. No statistically significant correlation was observed for MTS5. Distribution of the certain TILs-correlated metabolites were compared between each MTS to investigate the further relationship between TILs and MTSs (Supplementary Fig. S3).
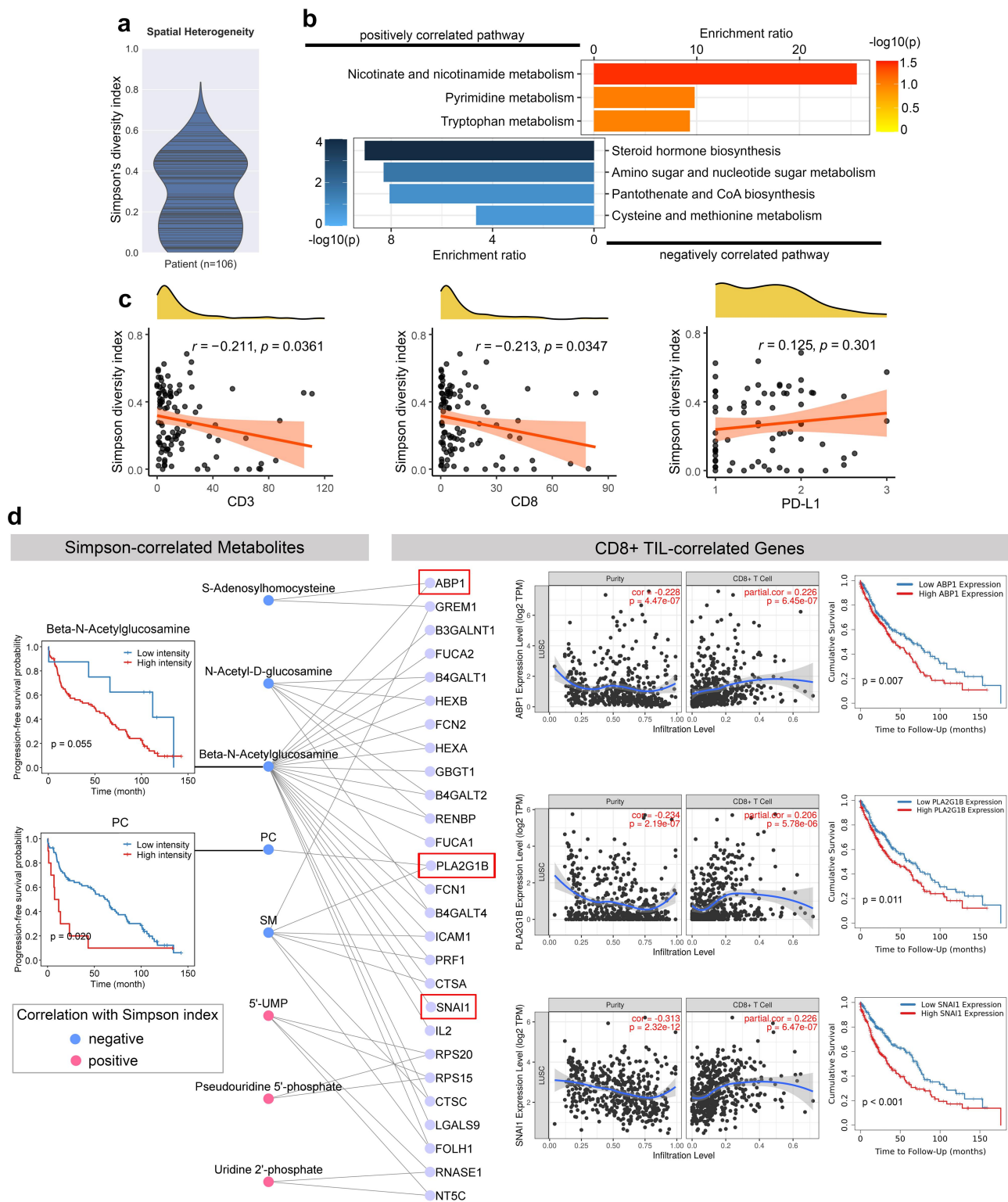
Figure 2. Metabolic heterogeneity evaluated by Simpson's diversity index was associated with TILs landscapes. (A) Distribution of Simpson's diversity index values in 106 LUSC patients. Each line represents one patient. Higher index indicates higher metabolic heterogeneity. (B) Distinct metabolic pathways were found to be correlated with Simpson's diversity index. (C) Simpson's diversity index was significantly correlated with the counts of CD3+ and CD8+ TILs but not the expression of PD-L1. (D) Metabolite-gene interaction network based on the metabolites associated with Simpson index in our cohort (*n* = 106) and genes associated with CD8+ TIL infiltration level in external validation cohort (*n* = 501). High expression of PC, *ABP1*, *PLA2G1B* and *SNAI1* were found to have unfavorable impact on PFS or OS of LUSC patients.

Multivariate Cox analysis among 5 MTSs with clinical factors for PFS and OS (Figure 5k) revealed that, MTS1 (CD3+CD8+) and MTS5 had significantly unfavorable impact on OS, while MTS1 (CD3+CD8+) and MTS4 (CD3+CD8+) had significantly unfavorable impact on PFS. MTS3 and MTS7 (PD-L1+) did not show independent prognostic potential.
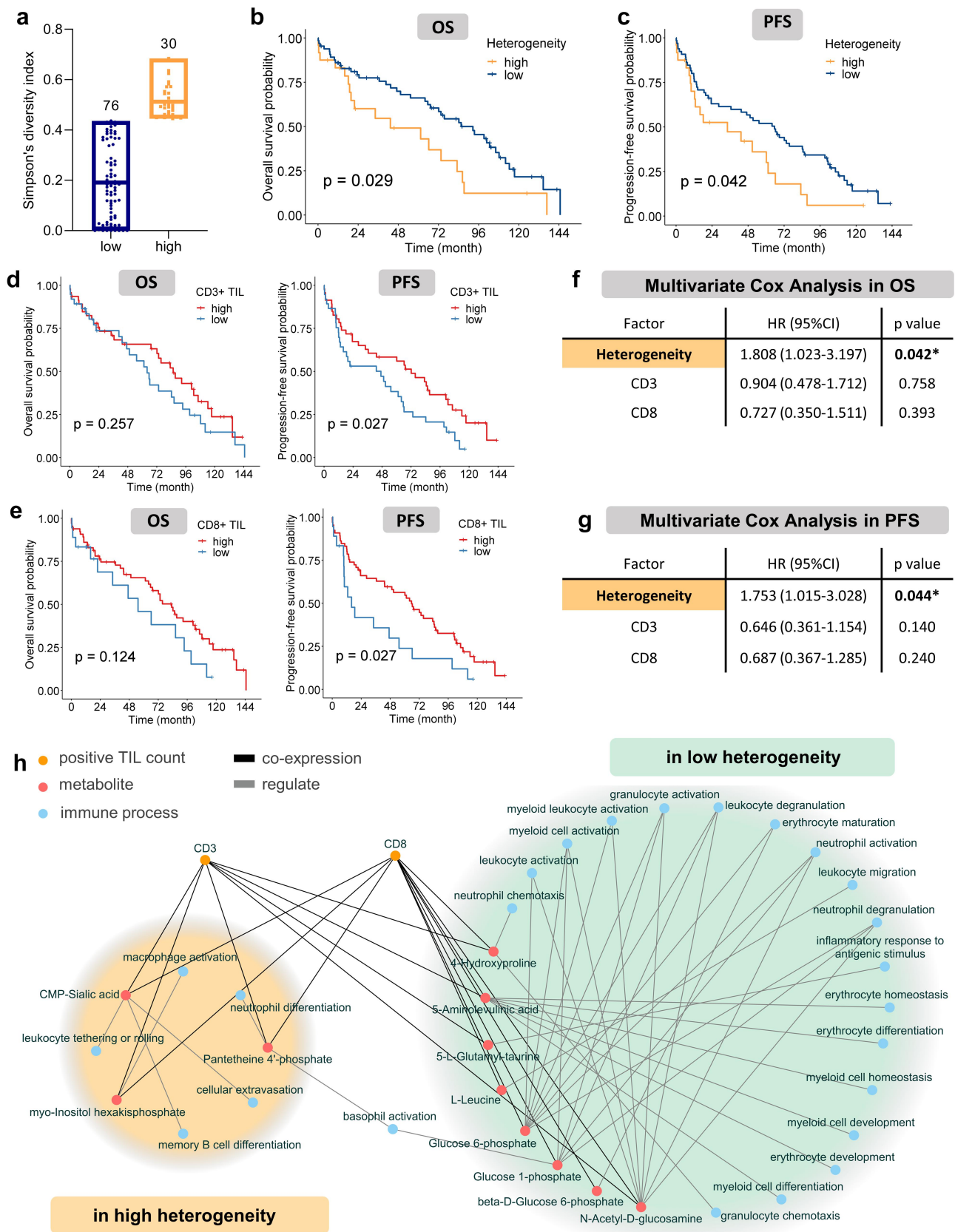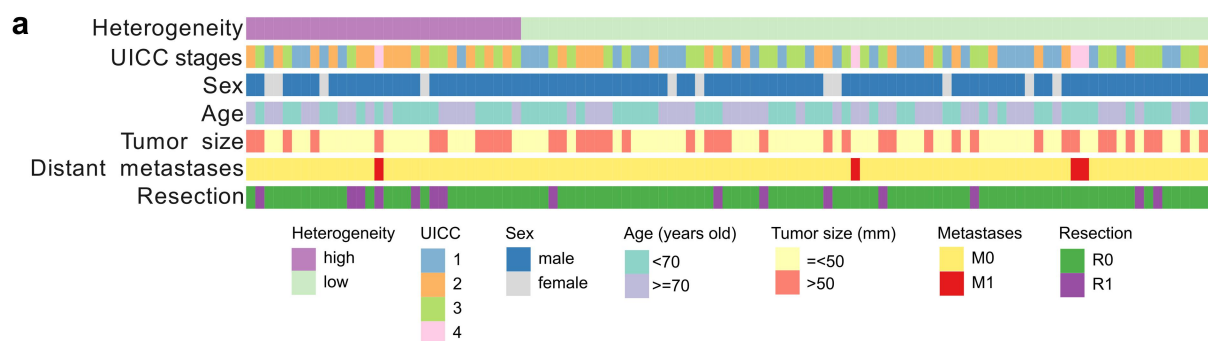
Figure 3. Association between metabolic heterogeneity and immunological landscapes were investigated. (A) Patients were classified into high- and low-heterogeneity levels by an optimized cutoff. Kaplan-Meier analysis of OS and PFS showed that (B-C) patients with high heterogeneity had significantly worse survival (high $n = 24$, low $n = 65$), and (D-E) patients with high CD3+ or CD8+ TIL had significantly better progression-free survival (CD3+: high $n = 46$, low $n = 37$; CD8+: high $n = 65$, low $n = 18$). (F-G) multivariate cox analysis demonstrated that metabolic heterogeneity was independent from CD3+ and CD8+ TIL to be a prognostic factor in both OS and PFS. (H) Network shows the metabolites-involved immune processes at high- and low-heterogeneity levels based on the CD3+ or CD8+ TILs co-abundant metabolites.

Figure 4. Metabolic heterogeneity was an independent prognostic factor. (A) Clinicopathological characteristics of 106 LUSC patients were visualized and their significance of differences between high- and low-heterogeneity were analyzed. (B) Multivariate cox analysis demonstrated that metabolic heterogeneity an independent prognostic factor in both OS and PFS.

MTSs were characterized by distinct metabolic pathways and responsiveness to chemotherapy

To compare the altered metabolic processes in MTSs, the metabolites closely associated with each MTS were subjected to metabolic pathway analysis, which in the meantime evaluated heterogeneity at the level of pathway. Figure 6a summarizes the major categories of identified pathways for five MTSs on the left and illustrated the detailed metabolic pathways and their correlations with each of five MTSs on the right. It is noteworthy that as independently prognostic factors, MTS1 (CD3+CD8+) exhibited positive association with carbohydrate metabolism and lipid metabolism; MTS4 (CD3+CD8+) and MTS5 exhibited negative association with carbohydrate metabolism and nucleotide metabolism, as well as positive correlation with amino acid metabolism and lipid metabolism.

Next, we mapped the metabolites closely correlated with each MTS to the SMPDB database for getting an insight of association between metabolites and chemotherapy. As demonstrated in the MTS-metabolite-drug network (Figure 6b), among all correlated metabolites, adenosine 5'-diphosphate (5'-ADP), adenosine 3',5'-diphosphate (3',5'-ADP), uridine diphosphate (UDP), glutathione were observed to play roles in several anti-cancer drug pathways. In details, MTS3 was positively correlated with the pathways of sorafenib, tamoxifen, doxorubicm, docetaxel, erlotinib,

vinblastine, paclitaxel, vindesine, vincristine and vinorelbine. MTS4 (CD3+CD8+) and MTS5 were negatively correlated with the pathways of sorafenib, tamoxifen, doxorubicm, docetaxel, erlotinib, vinblastine, paclitaxel, vindesine, vincristine, and vinorelbine. MTS7 (PD-L1+) was positively correlated with the pathways of cyclophosphamide (Figure 6b).

Discussion

In this study, we explored tumor heterogeneity and immunometabolism in LUSC using high-resolution spatial metabolomics. We uncovered significant metabolic heterogeneity in LUSC tissues, finding that higher heterogeneity correlates with T cell suppression and poorer patient survival. By integrating genomics with metabolomics, we identified genes linked to metabolites and TILs, forming a metabolism-immune-gene connection. We defined five distinct metabolic tumor subpopulations, three of which were independently associated with poor prognosis. This is the first study to investigate the relationship between metabolic heterogeneity and the immunological landscape in LUSC.

It is known that the tumor metabolic microenvironment can suppress T cells, as those isolated from tumors often show signs of exhaustion and distinct metabolic signatures.[36,37] In LUSC tissues, we observed a negative correlation between CD3 + and CD8+ TILs and metabolic heterogeneity. This suggests competition for nutrients in the tumor microenvironment,
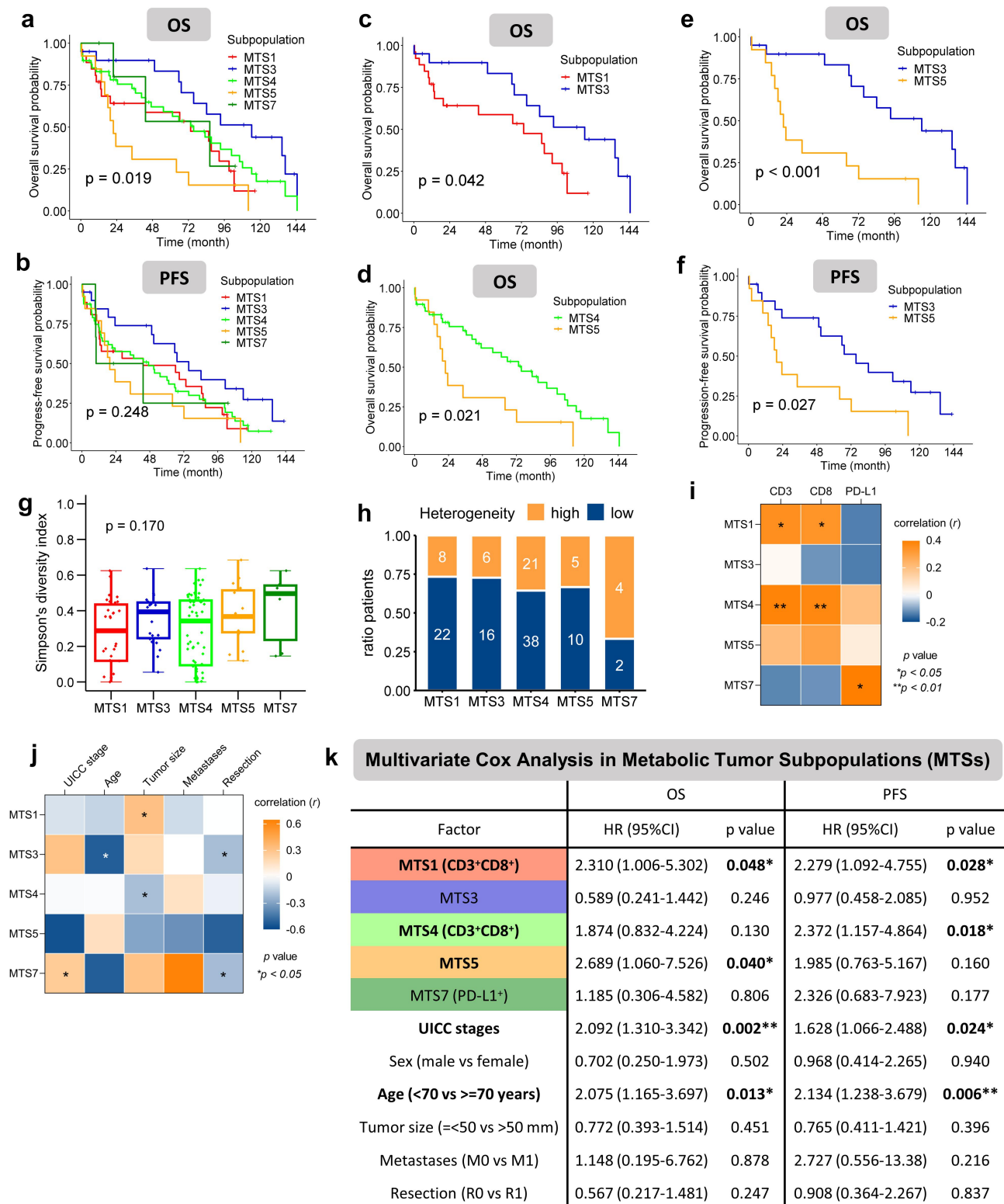
Figure 5. Association between MTSs and clinical features as well as TILs were investigated. (A-B) Kaplan-Meier analysis showed a significant difference among OS of all MTSs. In pairwise comparison, there were significant differences in OS between MTS1 and MTS3 (C), MTS4 and MTS5 (D), MTS3 and MTS5 (E), and in PFS between MTS3 and MTS5 (F). (G) Distribution of Simpson index of patients in each MTS. (H) Patients ratio of high- and low-heterogeneity levels in each MTS. (I) Significant positive correlations were found between MTS1 and MTS4 with CD3+ and CD8+ TILs counts, as well as between MTS7 and the expression of PD-L1. (J) MTSs correlated to different clinical features. (K) Multivariate cox analysis demonstrated that MTS1, MTS4 and MTS5 had independent prognostic value.

impairing TILs and aiding tumor progression.[36,38,39] It could be a possible explanation for our result that LUSC patients with higher heterogeneity were found to contain less TILs and had worse survival. What's more, metabolic heterogeneity showed an independent and stronger unfavorable impact on survival compared to TILs. Disruption of T cell activation due to altered tumor cell metabolism and other metabolic features in the TME indicates that this is an important mechanism for immunosuppression. On this basis, we can also reconsider that the constitutes of metabolic heterogeneity and immunity in
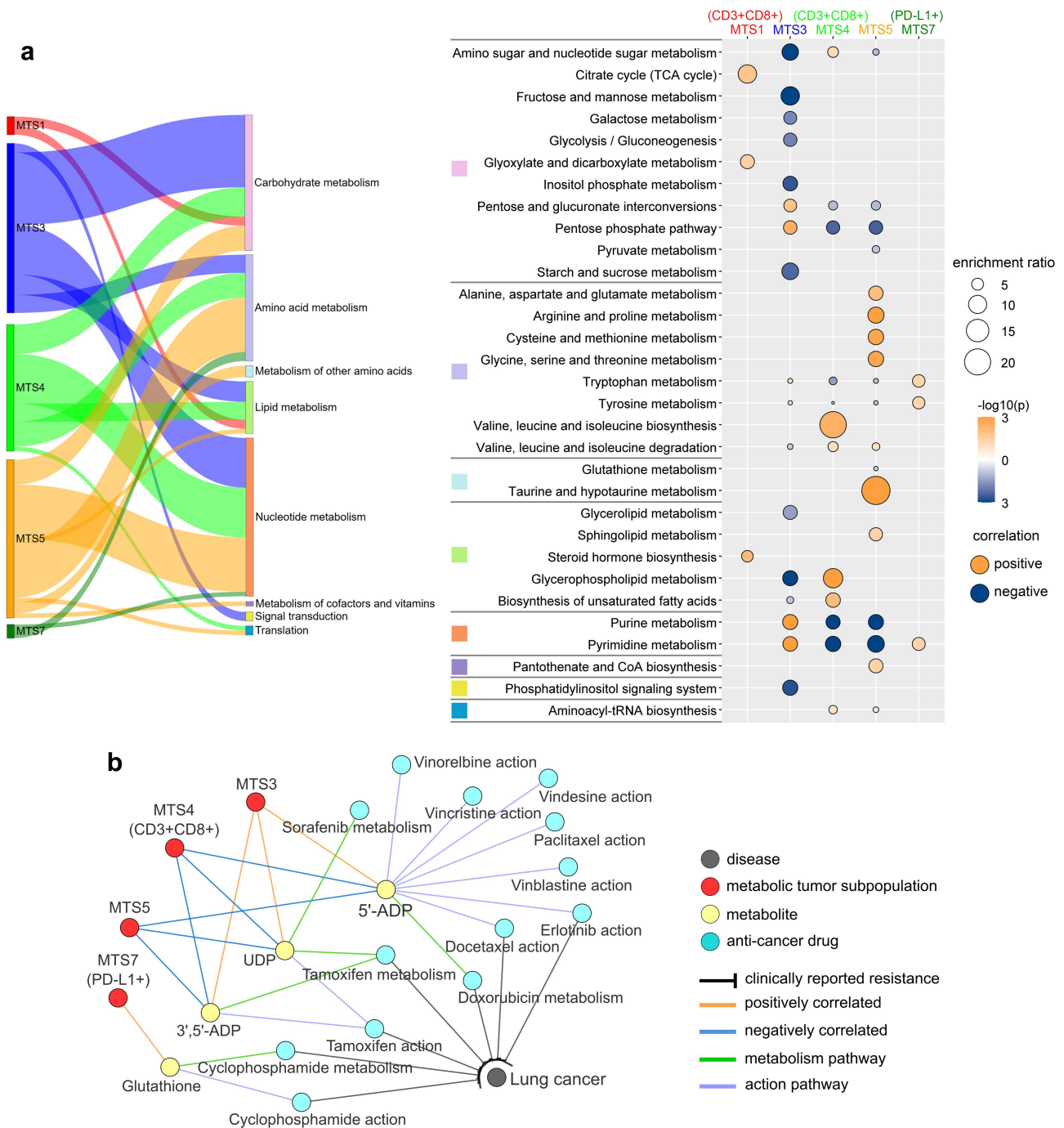
Figure 6. Mts-specific metabolite characteristics and pathways enrichment. (A) Variations of MTSs based on the metabolic pathway enrichment analysis. The major categories of associated pathways with each MTSs were shown by the left Sankey diagram. The width of flow represents the number of mapped metabolites. The detailed correlations between pathways and MTSs were illustrated in the right scatter plot. (B) Association of anti-cancer drug pathways with MTS.

subpopulations displaying distinct TIL features may enable the sensitivity or resistance to the specific therapy. It also implies that TILs are not distributed at random manner but closely associated with the metabolites constitution. Our comprehensive characterization of immunometabolism may provide new insights for further exploration of resistance mechanisms and optimization of immunotherapy strategies.

The tumor immune microenvironment as characterized by infiltration of CD8+ TILs and PD-L1 expression has been associated with the efficacy of immune checkpoint inhibitors (ICIs).[40,41] A thorough interrogation of the immunological

landscape is crucial for immunotherapy strategy selection and prediction of clinical responses in LUSC patients. We identified a metabolic tumor subpopulation, MTS4, which was positively associated with CD3+ and CD8+ TILs and showed independent prognostic value in LUSC. Our analysis suggests that ATP-ADP mediated catalysis and the effectiveness of erlotinib may be reduced in MTS4 (CD3+CD8+). Antibodies targeting PD1 or PD-L1 have achieved substantial overall survival improvements in advanced NSCLC, although major challenges still remain, including low response rate in unselected patients, lack of reliable predictive biomarkers, and

identification of more immunotherapeutic targets. Additionally, our findings indicate that MTS7, a subpopulation positively correlated with PD-L1 expression, may show enhanced sensitivity to cyclophosphamide. A previous study concluded that the LUSC patients with high tumor PD-L1 expression tend to resistant to ICIs therapy.[40] Taken together, for patients in MTS7 (PD-L1+), chemotherapy with cyclophosphamide could potentially be more effective than immunotherapy. Those findings may bring more insights for explaining the chemotherapy resistance mechanism of LUSC patients and improving the therapeutic strategies targeting different subpopulations.

Recent studies have linked cancer heterogeneity to tumor growth and treatment response.[42,43] In our spatial metabolic profiling of LUSC, we identified distinct metabolic pathways associated with different heterogeneity levels and subpopulations. Increased metabolism of nucleotides including purine and pyrimidine is acknowledged a hallmark of cancer, supporting uncontrolled growth of tumors.[44,45] Notably, pyrimidine metabolism was enhanced in patients with higher heterogeneity, correlating with worse survival and T cell suppression. Nucleotide metabolism was positively correlated with MTS3 and MTS7 (PD-L1+) but negatively with MTS4 (CD3+CD8+). Interestingly, tryptophan metabolism pathway was observed a positive correlation with metabolic heterogeneity, which means that the LUSC patients with higher heterogeneity might have enhanced tryptophan metabolism. Increased tryptophan catabolism in TME can mediate immunosuppressive effect on T cells, while decreased tryptophan catabolism was associated with a marked increase in the tumor infiltration and proliferation of polyfunctional CD8+ lymphocytes.[46,47]

As an independent prognostic factor, the subpopulation MTS5 in our study was found major abundant activities of amino acid metabolism and potentially resist to most chemotherapy drugs. Previously, activated amino acid metabolism was demonstrated to generate apatinib resistance by reprograming glutamine metabolism in NSCLC.[48] Furthermore, a growing body of evidence now supports the concept that targeting nucleotide metabolism can increase the antitumor immune response and enhance cancer immunotherapy.[49] While, MTS5 showed decreased activities of nucleotides metabolism and had no significant immune features observed. Taken above, the patients in MTS5 might face more unfavorable prognosis compared to other LUSC patients, due to a high possibility of resistance to chemotherapy and immunotherapy. Besides, we suppose that LUSC patients in MTS3 and MTS7 (PD-L1+) might show better response to the chemotherapy treatment that targets nucleotides metabolism, while the patients in the MTS4 (CD3+CD8+) with prognostic value and MTS5 might tend to be resistant to such treatment. In clinics, agents inhibiting synthesis and incorporation of nucleotides in DNA are widely used as chemotherapeutics to reduce tumor growth, cause DNA damage, and induce cell death.[50] Therefore, considering the suppression effect of tryptophan catabolism on immune immunity, blocking tryptophan catabolism with indoleamine 2,3-dioxygenase (IDO) inhibitors could be considered a prioritized treatment strategy for the LUSC patients with high metabolic heterogeneity, or those patients in subpopulation MTS7 (PD-L1+) that was also positively correlated to tryptophan metabolism. Chemotherapy, radiotherapy, and targeted therapy alter tumor metabolism, and metabolic changes are often implicated in treatment resistance.[51,52] Cancer patients elicit very individualized responses to different treatments. This situation demands better characterization of the whole tumor ecosystem. That is to say, the identification and effective targeting of molecular alterations in more specific subtypes of LUSC patients could further improve the treatment efficiency.

CD8+ TILs are key mediators of antitumor immunity and are strongly linked to survival in solid tumors.[53] We identified several genes interacting with metabolites and CD8+ TILs by integrating metabolic profiling with genomics in LUSC. High expressions of PLA2G1B, SNAI1, and ABP1 were associated with high CD8+ TIL levels and worse survival in a validation cohort of 501 LUSC patients. PLA2G1B, a phospholipase, may modulate lung inflammation.[54,55] SNAI1, an EMT transcription factor, is linked to chemotherapy resistance.[56,57] ABP1, less studied in human diseases, was found a potential role in our study in LUSC involving metabolic tumor heterogeneity and immune infiltrating landscapes.

An emerging view regarding cancer metabolism is that it is heterogeneous and context-specific. In our study, "metabolic heterogeneity" refers to the variation in metabolic activity that occurs within different regions of a tumor or between different cells within the same tumor, in particular lung tumor. The metabolic heterogeneity was reflected by the clustering among patient samples of lung cancer, and the complexity was further verified at the metabolic profiling level. This study highlights the existence of distinct metabolic tumor subpopulations within lung squamous cell carcinoma and each patient has a certain level of the metabolic profiling variation. These subpopulations or certain patients may exhibit different metabolic profiles, contributing to variations in immune cell infiltration, treatment response, and patient survival. This concept is central to understanding how different areas within a tumor may respond differently to therapies, especially those targeting metabolic pathways.

This study has some limitations inherent to the methodologies used. Specifically, the IHC antibodies are incompatible with the MALDI-MSI matrix, making it impossible to perform the two experiments on consecutive tissue sections. As a result, precise co-registration between IHC and spatial metabolomics data could not be achieved. Furthermore, the lack of direct co-localization between tumor-infiltrating lymphocytes (TILs) and metabolite distributions limits the ability to draw definitive spatial conclusions. Despite these challenges, the combined use of IHC and spatial metabolomics provides valuable insights into the interplay between immune cells and metabolic pathways. Future studies leveraging advanced imaging techniques or alternative co-registration methodologies could further refine this analysis and overcome these limitations.

Together, we provide a novel perspective for unraveling the metabolic heterogeneity and its association with immunology in LUSC. Our findings demonstrated that higher metabolic tumor heterogeneity foreshadows worse survival and revealed a strong connection between metabolic heterogeneity with TILs. The spatial metabolomics has opened the door to describe the complexity of lung cancer immunometabolism. Our comprehensive depiction

of the tumor heterogeneity-related immune landscapes and definition of distinct metabolic subpopulations could help design personalized treatment for LUSC patients in clinical practice.

Disclosure statement

No potential conflict of interest was reported by the author(s).

Funding

Authors' contributions

AW, SB, QW and NS conceptualized the study. QW performed data analysis and wrote the original manuscript. SB and PZ provided the tissue samples, clinical data, and immunological data. TK, AF and NS performed the MALDI FT-ICR MSI experiment. QW and CYZ contributed to the bioinformatics analysis and data visualization. AW, SB and QW obtained the fundings. All authors contributed to review and approval of the manuscript.

Data availability statement

All data and material are available within the article and its supplementary information file. Further related information could be accessed from the corresponding authors upon reasonable request.

Ethics statement

The study was conducted in accordance with the Declaration of Helsinki, and the local ethics committee of the Canton of Bern approved the study and waived the requirement for written informed consent (KEK 200/14).

References

1. Vander Heiden MG, DeBerardinis RJ. Understanding the intersections between metabolism and cancer biology. Cell. 2017;168 (4):657–669. doi:10.1016/j.cell.2016.12.039.

2. Buck MD, Sowell RT, Kaech SM, Pearce EL. Metabolic instruction of immunity. Cell. 2017;169(4):570–586. doi:10.1016/j.cell.2017.04.004.

3. Ayres JS. Immunometabolism of infections. Nat Rev Immunol. 2020;20(2):79–80. doi:10.1038/s41577-019-0266-9.

4. Makowski L, Chaib M, Rathmell JC. Immunometabolism: from basic mechanisms to translation. Immunol Rev. 2020;295(1):5–14. doi:10.1111/imr.12858.

5. Lim AR, Rathmell WK, Rathmell JC. The tumor microenvironment as a metabolic barrier to effector T cells and immunotherapy. Elife. 2020;9:9. doi:10.7554/eLife.55185.

6. Tabas I, Bornfeldt KE. Intracellular and intercellular aspects of macrophage immunometabolism in atherosclerosis. Circ Res. 2020;126(9):1209–1227. doi:10.1161/CIRCRESAHA.119.315939.

7. Turbitt WJ, Buchta Rosean C, Weber KS, Norian LA. Obesity and CD8 T cell metabolism: implications for anti-tumor immunity and cancer immunotherapy outcomes. Immunol Rev. 2020;295 (1):203–219. doi:10.1111/imr.12849.

8. Buck MD, O'Sullivan D, Pearce EL. T cell metabolism drives immunity. J Exp Med. 2015;212(9):1345–1360. doi:10.1084/jem.20151159.

9. Elia I, Haigis MC. Metabolites and the tumour microenvironment: from cellular mechanisms to systemic metabolism. Nat Metab. 2021;3(1):21–32. doi:10.1038/s42255-020-00317-z.

10. Liu Y, Zhang J, Li L, Yin G, Zhang J, Zheng S, Cheung H, Wu N, Lu N, Mao X, et al. Genomic heterogeneity of multiple synchronous lung cancer. Nat Commun. 2016;7(1):13200. doi:10.1038/ncomms13200.

11. Hensley CT, Faubert B, Yuan Q, Lev-Cohain N, Jin E, Kim J, Jiang L, Ko B, Skelton R, Loudat L, et al. Metabolic heterogeneity in human lung tumors. Cell. 2016;164(4):681–694. doi:10.1016/j.cell.2015.12.034.

12. Junttila MR, de Sauvage FJ. Influence of tumour micro-environment heterogeneity on therapeutic response. Nature. 2013;501(7467):346–354. doi:10.1038/nature12626.

13. Yuan Y. Spatial heterogeneity in the tumor microenvironment. Cold Spring Harb Perspect Med. 2016;6(8). doi:10.1101/cshperspect.a026583.

14. Dagogo-Jack I, Shaw AT. Tumour heterogeneity and resistance to cancer therapies. Nat Rev Clin Oncol. 2018;15(2):81–94. doi:10.1038/nrclinonc.2017.166.

15. Siegel RL, Miller KD, Fuchs HE, Jemal A. Cancer statistics, 2022. CA Cancer J Clin. 2022;72(1):7–33. doi:10.3322/caac.21708.

16. Herbst RS, Morgensztern D, Boshoff C. The biology and management of non-small cell lung cancer. Nature. 2018;553 (7689):446–454. doi:10.1038/nature25183.

17. Heist RS, Sequist LV, Engelman JA. Genetic changes in squamous cell lung cancer: a review. J Thorac Oncol. 2012;7(5):924–933. doi:10.1097/JTO.0b013e31824cc334.

18. Jamal-Hanjani M, Wilson GA, McGranahan N, Birkbak NJ, Watkins TBK, Veeriah S, Shafi S, Johnson DH, Mitter R, Rosenthal R, et al. Tracking the evolution of non–small-Cell lung cancer. N Engl J Med. 2017;376(22):2109–2121. doi:10.1056/NEJMoa1616288.

19. Nahar R, Zhai W, Zhang T, Takano A, Khng AJ, Lee YY, Liu X, Lim CH, Koh TPT, Aung ZW, et al. Elucidating the genomic architecture of Asian egfr-mutant lung adenocarcinoma through multi-region exome sequencing. Nat Commun. 2018;9(1):216. doi:10.1038/s41467-017-02584-z.

20. Wu F, Fan J, He Y, Xiong A, Yu J, Li Y, Zhang Y, Zhao W, Zhou F, Li W, et al. Single-cell profiling of tumor heterogeneity and the microenvironment in advanced non-small cell lung cancer. Nat Commun. 2021;12(1):2540. doi:10.1038/s41467-021-22801-0.

21. Mogilenko DA, Sergushichev A, Artyomov MN. Systems immunology approaches to metabolism. Annu Rev Immunol. 2023;41 (1):317–342. doi:10.1146/annurev-immunol-101220-031513.

22. Ma X, Fernández FM. Advances in mass spectrometry imaging for spatial cancer metabolomics. Mass Spectrom Rev. 2022;43 (2):235–268. doi:10.1002/mas.21804.

23. Cao P, Wu S, Guo W, Zhang Q, Gong W, Li Q, Zhang R, Dong X, Xu S, Liu Y, et al. Precise pathological classification of non-small cell lung adenocarcinoma and squamous carcinoma based on an integrated platform of targeted metabolome and lipidome. Metabolomics. 2021;17(11):98. doi:10.1007/s11306-021-01849-5.

24. Shen J, Sun N, Zens P, Kunzke T, Buck A, Prade VM, Wang J, Wang Q, Hu R, Feuchtinger A, et al. Spatial metabolomics for evaluating response to neoadjuvant therapy in non-small cell lung cancer patients. Cancer Commun (Lond). 2022;42 (6):517–535. doi:10.1002/cac2.12310.

25. Buchberger AR, DeLaney K, Johnson J, Li L. Mass spectrometry imaging: a review of emerging advancements and future insights. Anal Chem. 2018;90(1):240–265. doi:10.1021/acs.analchem.7b04733.

26. Aichler M, Walch A. MALDI imaging mass spectrometry: current frontiers and perspectives in pathology research and practice. Lab Invest. 2015;95(4):422–431. doi:10.1038/labinvest.2014.156.

27. Neumann JM, Freitag H, Hartmann JS, Niehaus K, Galanis M, Griesshammer M, Kellner U, Bednarz H. Subtyping non-small cell lung cancer by histology-guided spatial metabolomics. J Cancer Res Clin Oncol. 2022;148(2):351–360. doi:10.1007/s00432-021-03834-w.

28. Kunzke T, Prade VM, Buck A, Sun N, Feuchtinger A, Matzka M, Fernandez IE, Wuyts W, Ackermann M, Jonigk D, et al. Patterns of carbon-Bound exogenous compounds in patients with lung cancer and association with disease pathophysiology. Cancer Res. 2021;81 (23):5862–5875. doi:10.1158/0008-5472.CAN-21-1175.

29. Vaysse PM, Heeren RMA, Porta T, Balluff B. Mass spectrometry imaging for clinical research – latest developments, applications, and current limitations. Analyst. 2017;142(15):2690–2712. doi:10.1039/C7AN00565B.

30. Ichinose J, Shinozaki-Ushiku A, Nagayama K, Nitadori J-I, Anraku M, Fukayama M, Nakajima J, Takai D. Immunohistochemical pattern analysis of squamous cell carcinoma: lung primary and metastatic tumors of head and neck. Lung Cancer. 2016;100:96–101. doi:10.1016/j.lungcan.2016.08.003.

31. Zhang H, AbdulJabbar K, Moore DA, Akarca A, Enfield KSS, Jamal-Hanjani M, Raza SEA, Veeriah S, Salgado R, McGranahan N, et al. Spatial positioning of immune hotspots reflects the interplay between B and T cells in lung squamous cell carcinoma. Cancer Res. 2023;83(9):1410–1425. doi:10.1158/0008-5472.CAN-22-2589.

32. Herbst RS, Baas P, Kim D-W, Felip E, Pérez-Gracia JL, Han J-Y, Molina J, Kim J-H, Arvis CD, Ahn M-J, et al. Pembrolizumab versus docetaxel for previously treated, PD-L1-positive, advanced non-small-cell lung cancer (KEYNOTE-010): a randomised controlled trial. Lancet. 2016;387(10027):1540–1550. doi:10.1016/S0140-6736(15)01281-7.

33. Thommen DS, Koelzer VH, Herzig P, Roller A, Trefny M, Dimeloe S, Kiialainen A, Hanhart J, Schill C, Hess C, et al. A transcriptionally and functionally distinct PD-1(+) CD8(+) T cell pool with predictive potential in non-small-cell lung cancer treated with PD-1 blockade. Nat Med. 2018;24(7):994–1004. doi:10.1038/s41591-018-0057-z.

34. Badoual C, Hans S, Merillon N, Van Ryswick C, Ravel P, Benhamouda N, Levionnois E, Nizard M, Si-Mohamed A, Besnier N, et al. PD-1–expressing tumor-infiltrating T cells are a favorable prognostic biomarker in HPV-Associated head and neck cancer. Cancer Res. 2013;73(1):128–138. doi:10.1158/0008-5472.CAN-12-2606.

35. Hanahan D, Weinberg RA. The hallmarks of cancer. Cell. 2000;100 (1):57–70. doi:10.1016/S0092-8674(00)81683-9.

36. Scharping NE, Menk AV, Moreci RS, Whetstone RD, Dadey RE, Watkins SC, Ferris RL, Delgoffe GM. The tumor microenvironment represses T cell mitochondrial biogenesis to drive intratumoral T cell metabolic insufficiency and dysfunction. Immunity. 2016;45(2):374–388. doi:10.1016/j.immuni.2016.07.009.

37. Gemta LF, Siska PJ, Nelson ME, Gao X, Liu X, Locasale JW, Yagita H, Slingluff CL, Hoehn KL, Rathmell JC, et al. Impaired enolase 1 glycolytic activity restrains effector functions of tumor-infiltrating CD8 + T cells. Sci Immunol. 2019;4(31):4(31. doi:10.1126/sciimmunol.aap9520.

38. Ho PC, Bihuniak J, Macintyre A, Staron M, Liu X, Amezquita R, Tsui Y-C, Cui G, Micevic G, Perales J, et al. Phosphoenolpyruvate is a metabolic checkpoint of anti-tumor T cell responses. Cell. 2015;162(6):1217–1228. doi:10.1016/j.cell.2015.08.012.

39. Chang CH, Qiu J, O'Sullivan D, Buck M, Noguchi T, Curtis J, Chen Q, Gindin M, Gubin M, van der Windt GW, et al. Metabolic competition in the tumor microenvironment is a Driver of cancer progression. Cell. 2015;162(6):1229–1241. doi:10.1016/j.cell.2015.08.016.

40. Yang M, Lin C, Wang Y, Chen K, Zhang H, Li W. Identification of a cytokine-dominated immunosuppressive class in squamous cell lung carcinoma with implications for immunotherapy resistance. Genome Med. 2022;14(1):72. doi:10.1186/s13073-022-01079-x.

41. Liu C, Zheng S, Lu Z, Wang Z, Wang S, Feng X, Wang Y, Sun N, He J. S100A7 attenuates immunotherapy by enhancing immunosuppressive tumor microenvironment in lung squamous cell carcinoma. Signal Transduct Target Ther. 2022;7(1):368. doi:10.1038/s41392-022-01196-4.

42. Luengo A, Gui DY, Vander Heiden MG. Targeting metabolism for cancer therapy. Cell Chem Biol. 2017;24(9):1161–1180. doi:10.1016/j.chembiol.2017.08.028.

43. Martinez-Outschoorn UE, Peiris-Pagés M, Pestell RG, Sotgia F, Lisanti MP. Cancer metabolism: a therapeutic perspective. Nat Rev Clin Oncol. 2017;14(1):11–31. doi:10.1038/nrclinonc.2016.60.

44. Buj R, Aird KM. Deoxyribonucleotide triphosphate metabolism in cancer and metabolic disease. Front Endocrinol (Lausanne). 2018;9:177. doi:10.3389/fendo.2018.00177.

45. Schneider G, Glaser T, Lameu C, Abdelbaset-Ismail A, Sellers ZP, Moniuszko M, Ulrich H, Ratajczak MZ. Extracellular nucleotides as novel, underappreciated pro-metastatic factors that stimulate purinergic signaling in human lung cancer cells. Mol Cancer. 2015;14(1):201. doi:10.1186/s12943-015-0469-z.

46. Qin R, Zhao C, Wang C-J, Xu W, Zhao J-Y, Lin Y, Yuan Y-Y, Lin P-C, Li Y, Zhao S, et al. Tryptophan potentiates CD8 + T cells against cancer cells by TRIP12 tryptophanylation and surface PD-1 downregulation. J Immunother Cancer. 2021;9(7):e002840. doi:10.1136/jitc-2021-002840.

47. Liang F, Wang G-Z, Wang Y, Yang Y-N, Wen Z-S, Chen D-N, Fang W-F, Zhang B, Yang L, Zhang C, et al. Tobacco carcinogen induces tryptophan metabolism and immune suppression via induction of indoleamine 2,3-dioxygenase 1. Signal Transduct Target Ther. 2022;7(1):311. doi:10.1038/s41392-022-01127-3.

48. Zhou X, Zhou R, Rao X, Hong J, Li Q, Jie X, Wang J, Xu Y, Zhu K, Li Z, et al. Activated amino acid response pathway generates apatinib resistance by reprograming glutamine metabolism in non-small-cell lung cancer. Cell Death Dis. 2022;13(7):636. doi:10.1038/s41419-022-05079-y.

49. Wu HL, Gong Y, Ji P, Xie Y-F, Jiang Y-Z, Liu G-Y. Targeting nucleotide metabolism: a promising approach to enhance cancer immunotherapy. J Hematol Oncol. 2022;15(1):45. doi:10.1186/s13045-022-01263-x.

50. Siddiqui A, Ceppi P. A non-proliferative role of pyrimidine metabolism in cancer. Mol Metab. 2020;35:100962. doi:10.1016/j.molmet.2020.02.005.

51. Butler EB, Zhao Y, Muñoz-Pinedo C, Lu J, Tan M. Stalling the engine of resistance: targeting cancer metabolism to overcome therapeutic resistance. Cancer Res. 2013;73(9):2709–2717. doi:10.1158/0008-5472.CAN-12-3009.

52. Morandi A, Indraccolo S. Linking metabolic reprogramming to therapy resistance in cancer. Biochim Biophys Acta Rev Cancer. 2017;1868(1):1–6. doi:10.1016/j.bbcan.2016.12.004.

53. Hwang WT, Adams SF, Tahirovic E, Hagemann IS, Coukos G. Prognostic significance of tumor-infiltrating T cells in ovarian cancer: a meta-analysis. Gynecol Oncol. 2012;124(2):192–198. doi:10.1016/j.ygyno.2011.09.039.

54. Tamaru S, Mishina H, Watanabe Y, Watanabe K, Fujioka D, Takahashi S, Suzuki K, Nakamura T, Obata J-E, Kawabata K, et al. Deficiency of phospholipase A2 receptor exacerbates ovalbumin-induced lung inflammation. J Immunol. 2013;191 (3):1021–1028. doi:10.4049/jimmunol.1300738.

55. Hui DY. Group 1B phospholipase A(2) in metabolic and inflammatory disease modulation. Biochim Biophys Acta Mol Cell Biol Lipids. 2019;1864(6):784–788. doi:10.1016/j.bbalip.2018.07.001.

56. Hsu DS, Lan H-Y, Huang C-H, Tai S-K, Chang S-Y, Tsai T-L, Chang C-C, Tzeng C-H, Wu K-J, Kao J-Y, et al. Regulation of excision repair cross-complementation group 1 by Snail contributes to cisplatin resistance in head and neck cancer. Clin Cancer Res. 2010;16(18):4561–4571. doi:10.1158/1078-0432.CCR-10-0593.

57. Dennis M, Wang G, Luo J, Lin Y, Dohadwala M, Abemayor E, Elashoff DA, Sharma S, Dubinett SM, St. John MA, et al. Snail controls the mesenchymal phenotype and drives erlotinib resistance in oral epithelial and head and neck squamous cell carcinoma cells. Otolaryngol Head Neck Surg. 2012;147(4):726–732. doi:10.1177/0194599812446407.